

MMiC: Mitigating Modality Incompleteness in Clustered Federated Learning

Lishan Yang
The University of Adelaide
Adelaide, Australia
lishan.yang@adelaide.edu.au

Wei Emma Zhang
The University of Adelaide
Adelaide, Australia
wei.e.zhang@adelaide.edu.au

Quan Z. Sheng
Macquarie University
Sydney, Australia
michael.sheng@mq.edu.au

Lina Yao
CSIRO's Data 61 and The University
of New South Wales
Sydney, Australia
lina.yao@data61.csiro.au

Weitong Chen
The University of Adelaide
Adelaide, Australia
weitong.chen@adelaide.edu.au

Ali Shakeri
The University of Adelaide
Adelaide, Australia
ali.shakeri@adelaide.edu.au

Abstract

In the era of big data, data mining has become indispensable for uncovering hidden patterns and insights from vast and complex datasets. The integration of multimodal data sources further enhances its potential. Multimodal Federated Learning (MFL) is a distributed approach that enhances the efficiency and quality of multimodal learning, ensuring collaborative work and privacy protection. However, missing modalities pose a significant challenge in MFL, often due to data quality issues or privacy policies across the clients. In this work, we present MMiC, a framework for Mitigating Modality incompleteness in MFL within the Clusters. MMiC replaces partial parameters within client models inside clusters to mitigate the impact of missing modalities. Furthermore, it leverages the Banzhaf Power Index to optimize client selection under these conditions. Finally, MMiC employs an innovative approach to dynamically control global aggregation by utilizing Markowitz Portfolio Optimization. Extensive experiments demonstrate that MMiC consistently outperforms existing federated learning architectures in both global and personalized performance on multimodal datasets with missing modalities, confirming the effectiveness of our proposed solution. Our code released at <https://github.com/gotobcn8/MMiC>.

CCS Concepts

• **Computing methodologies** → *Distributed computing methodologies*; **Distributed artificial intelligence**; **Machine learning**; • **Information systems** → *Data mining*.

Keywords

Federated Learning, Multimodal Learning, Missing Modality

ACM Reference Format:

Lishan Yang, Wei Emma Zhang, Quan Z. Sheng, Lina Yao, Weitong Chen, and Ali Shakeri. 2025. MMiC: Mitigating Modality Incompleteness in Clustered Federated Learning. In *Proceedings of the 34th ACM International Conference on Information and Knowledge Management (CIKM '25)*, November 10–14, 2025, Seoul, Republic of Korea. ACM, New York, NY, USA, 11 pages. <https://doi.org/10.1145/3746252.3761140>

1 Introduction

Federated Learning (FL), introduced by McMahan et al. [29], enables multiple participants to collaboratively train a unified model without sharing raw data, thus preserving privacy. This paradigm is particularly well-suited for applications such as medical image analysis, connected vehicles, blockchain and so on [18, 26, 33]. However, the absence of data sharing in FL introduces significant challenges, including model heterogeneity, communication overhead, and data distribution disparities.

Multimodal Federated Learning (MFL) extends the FL paradigm to multimodal tasks, which leverage the complementary nature of multiple data modalities (e.g., text, images, and audio) to achieve superior performance on large-scale datasets. However, a common challenge in MFL is modal incompleteness, where certain modalities may be missing for some clients due to hardware limitations or data collection constraints. This issue can significantly degrade model performance, especially in heterogeneous scenarios. Existing approaches to tackling missing modalities primarily concentrate on two main aspects: the Data Processing Aspect, which involves generating absent modalities or their representations from the available ones, and the Strategy Design Aspect, which entails devising flexible model architectures capable of adapting to a variable number of available modalities during training, such as attention-based models [50]. While these methods have shown promise, they are often limited to specific models or datasets. For instance, Yu et al. [55] proposed a specialized LSTM-based model to handle incomplete modalities, but such solutions are not easily generalizable to other complex multimodal tasks because they rely heavily on the specific architecture. Moreover, the lack of a unified approach to address modality incompleteness across diverse tasks and datasets further restricts their applicability in broader real-world scenarios. In addition, the current MFL algorithm is limited to information

Permission to make digital or hard copies of all or part of this work for personal or classroom use is granted without fee provided that copies are not made or distributed for profit or commercial advantage and that copies bear this notice and the full citation on the first page. Copyrights for components of this work owned by others than the author(s) must be honored. Abstracting with credit is permitted. To copy otherwise, or republish, to post on servers or to redistribute to lists, requires prior specific permission and/or a fee. Request permissions from permissions@acm.org.
CIKM '25, Seoul, Republic of Korea.

© 2025 Copyright held by the owner/author(s). Publication rights licensed to ACM.
ACM ISBN 979-8-4007-2040-6/2025/11
<https://doi.org/10.1145/3746252.3761140>

exchange between clients and the server, lacking interaction between clients. For instance, PmcmFL [1] compensates for missing modality through server aggregation prototypes. However, due to constraints such as Non-IID data, the aggregated prototypes may not be suitable for all clients.

Clustered Federated Learning (CFL), a specialized form of FL Personalization [45], groups clients into clusters based on models, parameters, or datasets. Collaborative training within each cluster reduces the impact of data distribution disparities between clients. Recent advancements in CFL, such as one-shot clustering methods like PACFL [47], leverage the decomposability of data to identify client clusters efficiently. Each cluster inherently contains clients with similarities in both data and model parameters. We can leverage this characteristic of federated clustering to improve the training scenarios involving missing modalities. This means that *the model parameters from clients within the same cluster that have full modalities can be used to fill in the parameters of clients with missing modalities*. Due to the constraints of communication efficiency within clusters, we can shrink replaced parameters to only one layer most significantly affected by the missing modalities.

Current CFL algorithms predominantly employ random client selection [12, 13, 40], which ensures fairness over multiple rounds of updates by granting each client an equal opportunity to participate in aggregation. However, we do not expect clients with severe missing modalities to enjoy the same level of aggregation rights. Therefore, by analyzing performance variations across client training rounds, we can determine whether a client is frequently affected by missing modalities. This allows us to adjust the probability of client selection accordingly.

Since the global model, due to the intermediate aggregation process involving the cluster-client hierarchy, cannot directly perceive changes in clients' missing modalities, we can employ certain functions or metrics to evaluate the training process within each cluster. This evaluation yields a specific value that can be reported to the server, enabling the server to determine the aggregation weights for the current round.

To achieve these goals, we propose MMiC, a framework that integrates our solutions for the three issues. In particular, we employ the rate of parameter variation to identify the parameters to be replaced. Moreover, the parameters from clients possessing complete modality data and belonging to the same cluster will be utilized to supplant those of clients with incomplete modality data. To enhance the current cluster client selection strategy in the presence of missing modalities, we incorporate the Banzhaf Power Index (BPI), a well-known coalitional game theory, to assess the contribution of each client. This approach enables us to preferentially select the clients who are more contributable, to perform more efficient and effective aggregation processes. We further make use of Markowitz Portfolio Optimization, a return-risk balancing asset optimization algorithm to assess the training process on clusters in a nonlinear manner compared to the standard weighted averaging [48]. The global model adjusts the weights of parameter updates based on the scores obtained from the clusters, thereby reducing the impact of missing modalities in local clients on the global model.

MMiC is model-independent allowing for integration with various multimodal base models. It is also modality-agnostic, enabling its application across diverse multimodal scenarios regardless of

the specific modalities involved. Our experiments demonstrate that MMiC significantly outperforms traditional FL and MFL algorithms in terms of both accuracy and stability. In summary, the main contributions of our work are as follows:

- We propose a parameter substitution mechanism based on clustered federated learning, to mitigate the impact of missing modalities during training.
- We enhance the random client selection strategy by integrating the Banzhaf Power Index to favor clients with more significant.
- We are the first to apply the Markowitz Portfolio Optimization theory to evaluate the training process by incorporating the evaluation results into the global aggregation process to mitigate the negative impact of missing modalities on the global server.

2 Related Works

2.1 Clustered Federated Learning (CFL)

Centralized federated learning trains a global model in a central server by aggregating gradients collected across numerous participating clients. Personalized federated learning (PFL) has sprung up designed to better suit the individual characteristics of each client to address the heterogeneity. PFL strategies like Multi-Task Learning, Personalization Layers and Clustered Federated Learning (CFL) have attracted considerable attention in the literature [27, 44, 45, 49].

The fundamental concept of CFL is to group clients based on the similarity of their model parameters, data, or gradients. CFL emphasizes improving cooperation within these clusters to optimize the performance of cluster-specific models, while also enhancing overall global model performance. Ghosh et al. [13] first introduced the architecture for CFL, and recommended clustering based on the similarity of model parameters. Fedsoft further advanced the iterative CFL by allowing a client to belong to multiple clusters, outperforming previous efforts. However, these methods incurred substantial resource consumption. One-shot clustering was then introduced by Dennis et al. [6] for more efficient clustering. Their proposed method efficiently determined clustering attribution, identifying the uniqueness of client metrics within complex federated architectures. Vahidian et al. [47] proposed a one-shot CFL algorithm based on data subspace clustering. They measured the similarity between clients by decomposing the dataset via Singular Value Decomposition (SVD). Our proposed MMiC framework is under the same setting as the one-shot CFL [47, 52] and extends it to multimodal scenarios with missing modalities.

2.2 Multimodal Federated Learning (MFL)

Multimodal Federated Learning (MFL) extends standard federated learning to address multimodal datasets on clients and global server.

Challenges and Advances in MFL. FedCMR is the first to address multimodal tasks, though it encountered challenges such as modality discrepancies and missing data. Recent works have made strides in tackling these issues [56]. Graph-based FL represents a special case of CFL, they could be used to handle the heterogeneous modality fusion. FedMSplit [4] employs a dynamic and multi-view graph structure to adaptively capture the correlations amongst

multimodal local models. AGHG [35] creates a global knowledge enhancer to extract information from different modalities. These works collectively provide a foundation for understanding the challenges and solutions in MFL [3].

MFL with Missing Modality. CACMRN [51] is the first FL framework to propose solutions for missing modalities. They aim to achieve modality **reconstruction** using existing multi-modal data by training multiple functionally diverse models. Yu et al. [54] aim to address the issue of missing modalities in cross-modal retrieval. Clients, each with distinct modalities, learn the representation information of specific modalities and upload it to the server for **contrastive learning**. Fed-Multimodal [10] is a multimodal benchmark built upon the FL algorithm. The work presented a range of models and datasets and proposed a method to initialize the missing modal vector as **zero**. PmcmFL [1] applied the common **prototype exchange** method of federated learning against Non-IID to the missing modality, and they store prototypes of all modalities for all classes from each client on the server. When encountering missing modalities, it utilizes the corresponding class-specific prototypes to fill in the representations. In contrast, our approach does not impose restrictions on the types of multimodal tasks, meaning that we do not require the use of specific models.

3 Clustered Federated Learning

Optimization Objective. Given a global server \mathcal{G} and K clients $\{c_i\}_1^K$, let \mathcal{D}_k over $\mathcal{X} * \mathcal{Y}$ be the local dataset of the k -th client c_k , with \mathcal{X} and \mathcal{Y} represent the data inputs and labels, $n_k = |\mathcal{D}_k|$ be the dataset size. Client aggregated weight is calculated as $w_k = \frac{n_k}{\sum_k n_k} \cdot c_k$ and \mathcal{G} possess the model θ_k and $\theta_{\mathcal{G}}$ respectively and the models are the same when initialized. In each round of federated training, on the client, it is to learn local model θ_k by minimizing the local empirical loss: $F_i(\theta_k) = \sum_{\xi \in \mathcal{D}_k} \frac{\ell(\theta_k, \xi)}{n_k}$. Where $\ell(\cdot, \cdot)$ is the pre-defined task-driven loss function and ξ represents sampled training data in a batch. The clusters are defined by partitioning K clients into M disjoint subsets. Different from traditional federated selection, clustered federated selection is refined to each cluster, and each round has client subset \mathcal{S}_m selected in \mathcal{M}_m . The weight of cluster m is usually calculated as $w_m = \frac{\sum_{k \in \mathcal{M}_m} n_k}{\sum_1^M \sum_{k \in \mathcal{M}_m} n_k}$. Therefore, the global objective function can be expressed as:

$$\min \sum_{m=1}^M \sum_{k \in \mathcal{M}_m} w_k \ell(\theta_k) \quad (1)$$

Model Aggregation. We obtain cluster models from clients' models by using **FedAvg** [23]: $\Theta_m = \sum_{k \in \mathcal{M}_m} w_k \theta_k$. Our method for aggregating cluster models into the global model is elaborated in Section 4.3.

4 Methodology

Figure 1 depicts the architecture of MMiC. The left part illustrates the overall architecture including the clients at the bottom, clusters in the middle, and the global server at the top.

Each cluster accommodates multiple clients, and each client hosts multimodal data with missing modalities locally. The cluster model is derived from the federated average aggregation (Section 3).

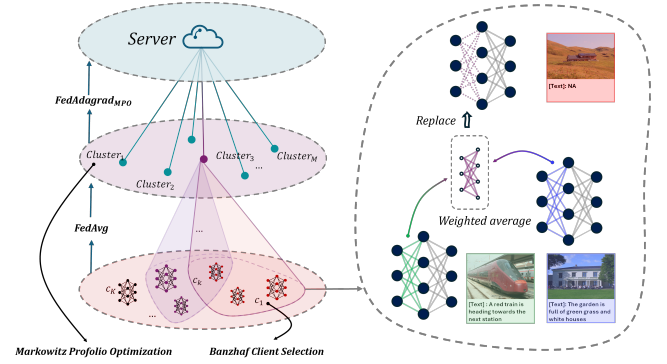


Figure 1: The MMiC architecture is divided into three layers: Server, Cluster, and Client. The right part illustrates the process of parameter substitution within a cluster. The MPO module primarily operates during the aggregation process from clusters to the global model, while the Banzhaf client selection is applied to the client selection within each cluster.

Within each cluster, MMiC handles the missing modality issue and the client selection task. First, a parameter layer substitution mechanism allows clients with missing modalities to obtain knowledge from clients with complete modality data within the same cluster (Section 4.1). Second, client selection is performed leveraging the Banzhaf Power Index, which identifies a set of *core* clients that contribute the most effectively to the cluster's model (Section 4.2).

For global aggregation, MMiC extends *FedAdagrad* [38] by adopting the Markowitz Portfolio Optimization (Section 4.3). This method incorporates client training evaluation results from each cluster and reduces the impact of missing modalities by down-weighting the contribution from clusters that contain missing modalities.

4.1 Cluster-based Parameter Substitution

We consider a multimodal setting where i -th data instance is a pair $\{X_i^{text}, X_i^{image}\}$. Missing modalities occur randomly, yielding samples such as $\{X_i^{null}, X_i^{image}\}$ or $\{X_i^{text}, X_i^{null}\}$ ¹.

To mitigate the consequences of missing modalities in each client, parameters that are less impacted by modality incompleteness are used to substitute those that are more significantly affected. We first propose a substitution strategy that can assist these clients in the training rounds. This strategy is inspired by the CFL setting, where a cluster model represents an aggregation of client models within the same cluster. The core idea is to substitute the parameters of client models with missing modality data with those of clients in the same cluster that have complete modality data. This approach involves two key tasks: (i) identifying the parameters to be substituted and (ii) ensuring the efficiency of the method.

Poverty Parameter Identification. In one round of client model training, we identify the layer that is the most affected by missing modalities as *poverty* layer. We use the parameter difference between the last batch $b-1$ and the current batch b to define the

¹Please note that MMiC is modality-agnostic – it remains effective regardless of the type or number of modalities, as long as modalities are consistent across clients. We have additional experiments on other modalities shown in Section 5.4

degree of this effect when the missing modality occurs in batch b and batch $b - 1$ is with complete modality²:

$$\rho_{k,t}^{e,b}(p) = \text{mean} \left(\left| \frac{\theta_{k,t}^{e,b}(p) - \theta_{k,t}^{e,b-1}(p)}{\theta_{k,t}^{e,b-1}(p)} \right| \right) \text{ and } \rho_{k,t}^{e,b}(p) \in \mathbb{R} \quad (2)$$

where e represents the epoch, t is the training round, k denote the client. $\rho_{k,t}^{e,b}(p)$ represents average parameter change rate of the p -th layer. As $\rho_{k,t}^{e,b}$ is a set containing all layers' change rates. We collect all the batches in the e -th epoch that contain complete modality data, while the preceding batch contains missing modality data, and form a batch set \mathcal{B}^* . Therefore, the relative change rate for the layer p in one epoch could be expressed as:

$$\rho_{k,t}^e(p) = \frac{\sum_{b \in \mathcal{B}^*} \rho_{k,t}^{e,b}(p)}{|\mathcal{B}^*|} \quad (3)$$

After calculating the average change rate for all layers in the model in one epoch, we identify the layer with the highest change rate across all epochs. This layer would be considered as the *poverty* layer with index $\mathcal{P}_{k,t}$:

$$\mathcal{P}_{k,t} = \arg \max_{p \in \{1,2,\dots,P\}} \rho_{k,t}(p) \quad (4)$$

It is worth mentioning that we select parameters from only one layer to reduce communication consumption.

Poverty Parameter Substitution (PPS). After identifying the poverty parameter in c_k , we propose to replace these parameters with the parameters from other clients in the cluster that have complete modality data. The proposed parameter substitution can be considered as a model editing strategy [24]. Specifically, we compute a weighted average of the corresponding parameters of other clients and replace the poverty parameter in c_k .

$$\theta_{k,t}(\mathcal{P}_{k,t}) = \sum_{j=1}^J w_j \theta_{j,t}(\mathcal{P}_{k,t}) \quad \text{where } \mathcal{P}_{j,t} = \emptyset, K + J = |\mathcal{M}_m| \quad (5)$$

where c_k represents the poverty client and c_j is the client that trained with the complete modality round, and both c_k and c_j belong to the cluster \mathcal{M}_m .

Optimizers Could Approximate Parameter Difference. Saving parameters between two batches is resource-intensive and time-consuming. However, we can roughly deduce the rate of change by utilizing the gradient derivation function of the optimizer. Below, we provide the calculation process for parameter variations during the Adam optimization processes. Here *momentum* is the bias-corrected moment estimate and \hat{v} is the second-moment estimate in Adam optimizer [20]:

$$\Delta \theta_{k,t}^{e,b} = \frac{\eta_{k,t} \text{abs}(\text{momentum}_b)}{\text{abs}(\theta_{k,t}^{e,b})(\sqrt{\hat{v}_b} + \epsilon)} \quad (6)$$

4.2 Banzhaf Client Selection in Clusters

The standard procedure for current CFL involves randomly selecting a subset of clients \mathcal{S}_m from each cluster for training in each

round, followed by a global aggregation. While the random selection is considered fair, there is a possibility that the cluster models aggregated by the selected clients may yield subpar results if some of the selected clients have a significant number of data instances with missing modalities. The negative impact will be transited to the global model through aggregation. Moreover, the negative impact will be enlarged over successive rounds of client training and cluster model aggregation, further degrading the performance of the global model.

Few CFL work addresses this issue and quantifies the impact of client selection for each cluster. We propose a novel method to fill the gap by leveraging Banzhaf Power Index [7, 21] (BPI) to select the core clients. It comprises two main steps. First, we identify core members within each subset selected in each round and tally the times of core members, denoted as *core times*. Then, by leveraging the historical selection times and core times, we devise a new client selection probability formula, which is applied in our subsequent client selection process. Banzhaf client selection does not require extra communication.

Core Members Identification. At training round t , each cluster \mathcal{M}_m makes a random client selection. We can obtain the i -th client's local model performance $a_{i,t}$ (i.e., accuracy, F1 score or RSum) of each client in the t -th round, and the performance $a_{i,t-1}$ in the $(t-1)$ -th round. We calculate the return $\alpha_{i,t}$ of the client for the t -th round based on the difference between these two rounds of performances as follows:

$$\alpha_{i,t} = a_{i,t} - a_{i,t-1} \quad (7)$$

where $\alpha_{i,t} < 0$ indicates that the client is generating a negative return to the *investment portfolio*; conversely, $\alpha_{i,t} > 0$ signifies a positive return. Then, the cluster's return is calculated as the sum of the client returns:

$$A_{\mathcal{S}_{m,t}} = \sum_{i=0}^{|\mathcal{S}_{m,t}|} w_i \alpha_{i,t} \quad (8)$$

For each cluster $\mathcal{S}_{m,t}$, we have its total return $A_{\mathcal{S}_{m,t}}$ by Equation (8). Correspondingly, we can calculate the total return for $\mathcal{S}'_{m,t}$ when excluding client c_i , $\mathcal{S}'_{m,t} = \mathcal{S}_{m,t} \setminus \{i\}$: Then, we use the return of cluster model to evaluate the core members:

$$c_i \text{ is core member? } \begin{cases} \text{True} & A_{\mathcal{S}_{m,t}} \geq \alpha_t^m \text{ and } A_{\mathcal{S}'_{m,t}} < \alpha_t^m \\ \text{False} & \text{otherwise} \end{cases} \quad (9)$$

The above equation describes the process of determining whether client c_i is a core member during the t -th round of client random selection. We utilize a *counter* $\phi(*)$ that starts with 0 to tally the number of times each client has been identified as a core member:

$$\phi(i) = \sum_{t=1}^T \mathbb{I}(c_i \text{ is a core member}) \quad (10)$$

where $\mathbb{I}(*)$ is the indicator function that returns 1 if the condition $*$ is satisfied, otherwise returns 0.

Client Selection Probability. BPI prioritizes clients without missing modalities, thus favoring those that contribute more to performance improvements. We could design a method to measure the probability of a client being selected in the current round based on its core times. Our goal is to ensure that a higher core time

²We are aware of the missing modality status of the data.

corresponds to a higher probability. However, this way will make clients with small core times unlikely to be selected later. To solve this problem, we set another counter $\mathcal{T}(\ast)$ that records the number of times the client has been selected in its history, and we determine the final selection probability by balancing the historically selected times $\mathcal{T}(i)$ and the core times $\phi(i)$:

$$\text{prob}(i) = \frac{e^{\frac{\tau\phi(i)}{\mathcal{T}(i)}}}{\sum_{i \in \mathcal{M}_m} e^{\frac{\tau\phi(i)}{\mathcal{T}(i)}}} \quad (11)$$

For client i in cluster \mathcal{M}_m , its probability in the t -th round to be selected is $\text{prob}(i)$. We increase the disparity in probability allocation for each client through an exponential function, where τ is a temperature constant. As τ increases, the disparity in probability increases, and as τ decreases, the disparity in probability decreases.

4.3 Markowitz Portfolio Optimization for Global Aggregation

In our framework, MMiC builds upon *FedAdagrad* [38] to support adaptive cluster-level aggregation in the presence of modality incompleteness. To enhance global robustness, we propose a novel integration of Markowitz Portfolio Optimization (MPO) into *FedAdagrad*.

Originally introduced in financial theory [30], MPO constructs investment portfolios that trade off expected **return** and associated **risk**. Inspired by this principle, we adapt the concept to dynamically regulate the influence of each cluster in global aggregation. Specifically, clusters consisting of underperforming clients—such as those suffering from missing modalities—may introduce biased or unreliable updates. We treat each cluster as an “investment” and aim to down-weight risky clusters while preserving beneficial contributions.

Our approach introduces a scoring function that quantifies the overall quality of a cluster’s update in each round, based on both its expected return and internal risk. This score directly informs the global aggregation process, enabling us to balance between current update quality and accumulated historical knowledge. To achieve this, we require three core indicators to construct our “*investment portfolio*” for cluster \mathcal{M}_m includes the expected return (i.e., payoff) of the cluster, denoted as $A_{m,t}$ (Equation 8); the risk $\bar{\sigma}_{m,t}$, derived from the intra-cluster covariance; and the return-risk tolerance coefficient λ that governs the trade-off between return and risk for the cluster.

Cluster Risk. According to the asset risk calculation formula from MPO [28, 30], we obtain the covariance as follows:

$$\bar{\sigma}_{m,t} = \sum_{i=1}^{|\mathcal{S}_m|} \sum_{j=1}^{|\mathcal{S}_m|} w_i w_j \left\{ \frac{1}{T-1} \sum_{t=1}^T (\alpha_{i,t} - \bar{\alpha}_{i,t-1})(\alpha_{j,t} - \bar{\alpha}_{j,t-1}) \right\} \quad (12)$$

where $\bar{\alpha}_{i,t-1}$ represents the historical average return for client i in round $t-1$. w_i and w_j are weights assigned to the i -th and j -th clients respectively (Please refer to Section 3 for weights’ calculation). Then the Risk-Adjusted Return Coefficient (**RARC**) is formulated as follows:

$$\gamma_{m,t} = \lambda \bar{\sigma}_{m,t} - (1 - \lambda) A_{m,t} \quad (13)$$

where $\lambda [0,1]$ is the risk tolerance constant. We defaultly set it as 0.5 to balance risk and return. Section 5.8 demonstrates how we reduce the cubic computational complexity of MPO to a quadratic complexity.

Participate in Global Aggregation. We have evaluated the training RARC $\gamma_{m,t}$ for each cluster. Next, we dynamically incorporate these RARC into the global aggregation process. A higher $\gamma_{m,t}$ indicates that the cluster has experienced a relatively poor local training process. In such scenarios, our objective is to diminish the impact of the current round’s parameter updates on the global aggregation by down-weighting the cluster parameters associated with higher $\gamma_{m,t}$.

To accomplish dynamic aggregation between current round and historical rounds, *FedAdagrad* employs the following update mechanism: $\Delta_{m,t}$ is the difference between the current cluster model and the global model. $mtn_{m,t}$ is updated iteratively and collects the historical parameter updates, while β balances the historical parameter updates $mtn_{m,t-1}$ and $\Delta_{m,t}$. A larger β indicates the retention of more historical parameter information. v_t is an accumulated squared change estimate used to measure changes in parameters and adjust the learning rate to improve the stability and convergence speed of the optimization process:

$$\begin{aligned} \Delta_{m,t} &= w_m (\Theta_{m,t} - \Theta_{\mathcal{G},t-1}) \\ mtn_{m,t} &= \beta mtn_{m,t-1} + (1 - \beta) \Delta_{m,t}, \beta \in [0, 1) \\ v_{m,t} &= v_{m,t-1} + \Delta_{m,t}^2 \\ \theta_{\mathcal{G},t} &= \theta_{\mathcal{G},t-1} + \eta \frac{mtn_{m,t}}{\sqrt{v_{m,t} + \tau}} \end{aligned} \quad (14)$$

We introduce a dynamic $\beta_{m,t}^*$ to replace the static β in *FedAdagrad*, which effectively captures the influence of $\gamma_{m,t}$:

$$\begin{aligned} \beta_{m,t}^* &= \beta + \frac{\tanh(\text{ReLU}(\gamma_{m,t}))}{\tau} \\ mtn_{m,t} &= \beta_{m,t}^* mtn_{m,t-1} + (1 - \beta_{m,t}^*) \Delta_{m,t}, \beta_{m,t}^* \in [0, 1) \end{aligned} \quad (15)$$

When $\gamma_{m,t} > 0$, then $\beta_{m,t}^* > \beta$, which helps retain more historical parameter updates in the global aggregation. Otherwise, $\beta_{m,t}^* = \beta$. Here τ serves as the smoothness control constant for the range. We suggest setting the temperature to range [10,20], and it depends on the value set for β .

4.4 Variants of MMiC

We propose two MMiC variants by extending two existing methods that address modality incompleteness. Specifically, by integrating these methods with the three proposed modules in Section 4.1 - 4.3, we form the two MMiC variants.

MMiC (Modality Reconstruction). In this variant, we adopt the reconstruction idea from [41] and incorporate two modality reconstruction models, Text-to-Image and Image-to-Text, at each cluster to reconstruct the missing modality using the data from the complete modality.

MMiC (GMC-Fusion). The other MMiC variant is based on the GMC-Fusion model [34]. This variant necessitates the additional projecting of information from two modalities into the shared space, followed by computing the Geometric Multimodal Contrastive loss

using all available modality representations and shared space representations from a batch. In this way, the missing modality information could be filled in the shared space.

5 Experiments

5.1 Experiment Setup

5.1.1 Datasets, Models and Metrics. Our evaluation of MMiC is based on two multimodal classification datasets and one multimodal retrieval dataset. Because each dataset has distinct characteristics, we followed [10, 16] in employing different base models, learning configurations and evaluation metrics for each dataset.

CrisisMMD [32]. It is a multi-modal dataset for classification consisting of 18,126 samples annotated tweets and images. We brought in a *lightweight multi-modal* model that used pre-trained embedding layers for input and concatenates shared representations [10, 15]. Following [10], we employed the F1 [14] score to evaluate the performance of CrisisMMD.

UPMC-Food101 [11]. UPMC-Food101 sourced from Food101, containing 101,000 image-text pairs across 101 food categories. We used *CLIP* with the official ViT version of the backbone pre-trained model [36]. We froze the first 11 layers of attention while retaining the last layer of attention and the final output linear layer for parameter updates. We employed accuracy to evaluate its performance.

Flickr30k [53]. It is an image captioning dataset for retrieval, which is comprised of 31,783 images and the corresponding captions. We used *SCAN* (Stacked Cross Attention Network) [22] as the multimodal retrieval model. SCAN is a model designed for image-text matching. We relied on the RSum as the evaluation metric to measure the performance of the retrieval task [8].

Learning settings. In all of our experiments, we set a global learning rate (0.1, 0.01, 0.05) in the three datasets (CrisisMMD, Food101, Flickr30k) respectively to global optimizers (both *FedAdagrad* and *FedAdagrad_{MPO}*). Our Parameter difference calculation process is derived from Equation 6 and we used the Adam optimizer with a learning rate of 0.005 for the clients. These parameters were obtained through our simple tuning in the early stage of our experiment. The batch size for the CrisisMMD dataset was set to 15, and 7 for the UPMC-Food101 dataset, 20 for the Flickr30k dataset. All the local epoch was set to 3. The loss function on the client was cross-entropy, except for MMiC (GMC-Fusion), where the loss consists of two parts: cross-entropy and contrastive loss between existing modalities [34].

5.1.2 Benchmark Algorithms. We compared MMiC with selected representative works and state-of-the-art works. **FedAvg [29]** (first work for FL), **FedOpt [39]** (outstanding FL work), **FedSoft [40]** (a soft SOTA clustered FL), **PACFL [47]** (an advanced CFL methodology), **CreamFL [54]** (MFL for addressing missing modality), and **PmcmFL [1]** (a SOTA work for addressing missing modality).

5.1.3 Cluster and Clients Settings. In this experiment, we employed two distance metrics for clustering: Locality Sensitive Hashing (LSH) sketch [25, 52] and SVD decomposition [47]. All experiments used the LSH sketch for clustering unless otherwise noted. Each cluster had a test set visible to all clients within the cluster. Additionally, the global server provided accessibility to the test set

for all clients. We simulated the Non-IID scenario by utilizing the *Dirichlet* distribution [46] with $\beta_{diri} = 0.5$. For all the experiments, we set the number of clients to 50 so that ensured each client had at least 200 training samples. Our client selection strategy comprised an initial phase of 100 rounds with random selection, followed by a subsequent phase of 200 rounds utilizing Banzhaf client selection (300 global rounds).

5.1.4 Missing Modality Settings. Our setting with missing modalities was governed by two variables: *clients with missing modality (mc)* and *missing modality rate (mm)*, denoting the proportion of all clients selected to have missing modalities and the proportion of missing samples on these clients, respectively. Our main experiment (Section 5.2) offered three levels of modality incompleteness settings: (mm@0.2, mc@0.3), (mm@0.2, mc@0.5) and (mm@0.5, mc@0.5). (mm@0.2, mc@0.3) means ratio of mm = 20% and ratio of mc = 30%. Each client has a fixed number of missing samples, determined by the *mm* rate. In each round, among the clients selected for aggregation, we use *mc* to decide whether the selected clients will activate missing data. Since the selected clients use a random training subset for training in each round, the maximum missing modality rate for a client in that round is $\min(\frac{\text{missing samples}}{\text{subset samples}}, 1)$.

5.2 Overall Performance

We evaluated MMiC based on *global performance (gbp)* and *personalized performance (plp)* and presented the results in Table 1. To do the evaluation, we made use of the global test dataset to evaluate the *global* model performance following [29], and adopted the weighted average performance from client models to evaluate the *plp* following [9]. MMiC and its two variants secure the top positions across all tasks and all missing modality scenarios. While MMiC (MR) excelled in classification tasks, being the only algorithm to achieve an F1 score exceeding 30 on CrisisMMD (mm@0.2, mc@0.5) at *gbp*. MMiC (GF) significantly outperformed all other algorithms in modality retrieval tasks across all three metrics. These results highlighted the superiority of MMiC in handling diverse missing modality scenarios.

FedOpt demonstrated strong *gbp* on the CrisisMMD dataset (mm@0.2, mc@0.3) and (mm@0.2, mc@0.5). FedSoft’s performance is medium across experiments with multiple missing modalities settings and datasets both in global and personalized evaluations. As a CFL algorithm, PACFL do not exhibit outstanding performance in *gbp*. In contrast, it demonstrated excellent performance in personalized evaluation. CreamFL is primarily an algorithm designed for retrieval tasks. The overall performance of CreamFL is relatively mediocre except for Flickr30k (mm@0.2, mc@0.5), their method ranked second in this setting both in global and personalized evaluations. PmcmFL currently supports only classification tasks; however, its performance in classification tasks is somewhat limited. Overall, MMiC consistently outperforms traditional methods for addressing missing modality challenges in FL.

5.3 Ablation Study

We conducted an ablation study on the CrisisMMD, Food101, and Flickr30k datasets under the settings of mm@0.2 and mc@0.5 (Table 2). The ablation modules are denoted as ‘b’, ‘p’, and ‘s’ (BPI, MPO

Table 1: Global and personalized performance compared with different algorithms. Bold with * indicated the best performance, while bold black indicated excellent or stable top three performance. Since the PmcmFL algorithm is only for classification tasks, it can't be compared in Flickr30k. MR stands for Modality Reconstruction and GF is GMC-Fusion.

Global	CrisisMMD (F1 score)			UPMC-Food101 (Accuracy)			Flickr30k (RSum score)		
	mm@0.2 mc@0.3	mm@0.2 mc@0.5	mm@0.5 mc@0.5	mm@0.2 mc@0.3	mm@0.2 mc@0.5	mm@0.5 mc@0.5	mm@0.2 mc@0.3	mm@0.2 mc@0.5	mm@0.5 mc@0.5
FedAvg [2017]	21.886 ± 2.87	20.531 ± 1.9	24.095 ± 0.178	88.053 ± 1.03	87.626 ± 1.34	88.283 ± 0.83	14.324 ± 1.68	4.704 ± 0.38	3.812 ± 0.16
FedOpt [2021]	29.320 ± 1.5	29.750 ± 2.04	26.292 ± 1.91	88.270 ± 0.53	89.064 ± 1.09	88.324 ± 0.85	16.138 ± 1.06	5.044 ± 0.61	12.576 ± 1.28
FedSoft [2022]	11.371 ± 0.02	8.180 ± 0.12	10.464 ± 0.01	87.471 ± 0.38	85.984 ± 0.79	81.461 ± 0.14	1.189 ± 0.01	1.297 ± 0.01	1.106 ± 0.02
PACFL [2023]	23.239 ± 3.35	20.274 ± 2.18	23.131 ± 3.029	88.152 ± 1.69	88.343 ± 1.31	88.439 ± 0.91	10.168 ± 1.14	8.013 ± 0.79	3.678 ± 0.25
CreamFL [2023]	22.766 ± 0.09	18.131 ± 1.0	16.958 ± 2.93	87.539 ± 0.26	87.102 ± 0.17	87.390 ± 0.88	13.965 ± 0.04	13.857 ± 0.06	11.839 ± 0.02
PmcmFL [2024]	24.610 ± 1.49	22.471 ± 0.44	22.946 ± 0.89	87.916 ± 0.90	85.159 ± 0.13	86.873 ± 0.52	-	-	-
MMiC	*29.462 ± 0.36	27.815 ± 1.44	*28.480 ± 1.86	88.777 ± 0.86	*89.436 ± 1.21	*89.428 ± 0.78	14.266 ± 1.20	8.322 ± 0.177	14.220 ± 1.28
MMiC (MR)	29.108 ± 0.86	*30.471 ± 0.77	28.354 ± 1.36	*88.997 ± 0.33	88.519 ± 2.31	89.044 ± 0.76	10.907 ± 1.21	10.152 ± 0.87	8.614 ± 0.84
MMiC (GF)	27.366 ± 2.22	26.229 ± 4.15	18.354 ± 2.06	88.465 ± 0.539	87.973 ± 1.26	89.056 ± 1.17	*18.333 ± 1.172	*25.418 ± 1.90	*22.707 ± 1.42
Personalized									
FedAvg [2017]	11.133 ± 0.49	9.671 ± 0.368	13.454 ± 0.87	77.039 ± 2.69	76.080 ± 1.47	75.786 ± 1.76	34.625 ± 2.39	17.625 ± 0.76	17.907 ± 0.24
FedOpt [2021]	17.417 ± 1.24	18.825 ± 0.16	15.205 ± 1.07	76.073 ± 2.05	76.492 ± 1.40	76.304 ± 2.76	40.275 ± 2.22	33.569 ± 1.89	43.152 ± 1.43
FedSoft [2022]	10.814 ± 0.384	8.012 ± 0.57	8.180 ± 0.01	75.547 ± 0.94	75.108 ± 1.21	73.918 ± 1.41	7.812 ± 1.32	6.103 ± 0.36	3.695 ± 2.52
PACFL [2023]	13.837 ± 1.72	10.454 ± 0.56	12.985 ± 1.97	83.805 ± 1.76	82.915 ± 1.75	83.722 ± 1.96	18.348 ± 0.62	20.171 ± 3.49	16.266 ± 1.08
CreamFL [2023]	11.169 ± 2.37	11.853 ± 0.815	11.338 ± 0.647	78.610 ± 0.411	78.484 ± 4.85	77.008 ± 2.07	76.900 ± 3.88	79.461 ± 1.92	75.122 ± 3.01
PmcmFL [2024]	17.010 ± 0.32	14.662 ± 1.36	14.048 ± 0.06	83.031 ± 1.20	81.673 ± 1.59	79.987 ± 0.82	-	-	-
MMiC	*19.936 ± 0.91	18.911 ± 1.13	18.259 ± 1.62	83.576 ± 0.75	*84.022 ± 1.19	84.057 ± 1.73	90.726 ± 3.28	75.814 ± 3.35	78.979 ± 2.38
MMiC (MR)	19.492 ± 0.27	19.174 ± 1.32	18.101 ± 1.08	83.519 ± 2.31	83.055 ± 3.74	82.948 ± 3.59	41.824 ± 6.70	33.388 ± 4.52	31.489 ± 4.17
MMiC (GF)	19.625 ± 4.797	*22.796 ± 6.04	*18.450 ± 2.73	*84.715 ± 3.13	83.639 ± 2.10	*84.601 ± 4.69	*112.506 ± 5.10	*160.99 ± 6.082	*124.414 ± 2.86

and PPS respectively). It shows that MMiC consistently achieves higher accuracy in the final rounds across multiple ablation tests. Specifically, 'w/o b' and 'w/o s' saw a decrease of more than 5% compared to MMiC in CrisisMMD while others still performed poorly. The final performance of 'w/o p' is close to MMiC, yet it remained approximately 2%, 0.2% and 3% lower than MMiC in three datasets respectively. In addition, removing any of the two contributions leads to varying degrees of performance decline, with the resulting performance consistently falling between that of MMiC and the configuration with a single module removed in Food101 and Flickr30k. We conclude that removing any module leads to performance degradation. We further proved the effectiveness of BPI in Section 5.5 and MPO in Section 5.6. We believe that BPI helps MMiC by reducing the weight of clients heavily affected by missing modalities, ensuring well-performing clients are prioritized. MPO further improves aggregation by minimizing the influence of high-risk clusters with missing modalities.

Table 2: Ablation study on CrisisMMD, Food101 and Flickr30k under (mm@0.2, mc@0.5).

Configuration	CrisisMMD (Acc)	Food101 (Acc)	Flickr30k (RSum)
w/o (b, p, s)	57.22	86.97	4.28
w/o s	58.91	88.54	6.99
w/o p	61.07	88.91	8.18
w/o b	57.03	87.26	8.10
only s	60.36	88.03	7.08
only p	59.87	87.49	4.84
only b	61.24	87.41	5.36
MMiC	63.55	90.12	11.02

5.4 Experiments on other modalities

In this section, we further broaden our experimental evaluation by incorporating more modalities, aiming to investigate the feasibility of our algorithm on non-dominant modalities, aiming to show that MMiC is modality-agnostic. UCI-HAR [37] and KU-HAR [43] both encompass smartphone sensor data utilized for the classification of diverse human activities. They include accelerometer and gyroscope readings gathered from a multitude of participants. We compared MMiC with FedOpt, which exhibited the good performance in Section 5.2, for this analysis. The experimental setup involved 30 clients running 150 global rounds, with all other parameters remaining consistent with those outlined in Section 5.1.3. The findings of this experiment are presented in Table 3. MMiC demonstrated a pronounced superiority over FedOpt, with enhancements of 2% and 6% in the KU-HAR and UCI-HAR respectively.

Table 3: Performance comparison of MMiC and FedOpt on UCI-HAR and KU-HAR datasets.

Dataset/Algorithm	MMiC (%)	FedOpt (%)
UCI-HAR (Acc)	86.99	75.83
KU-HAR (Acc)	80.89	73.24

5.5 Effectiveness of Banzhaf Client Selection

The federated architecture had shown the feasibility of client selection, as demonstrated in [5, 31]. In this section, we compared training efficiency under missing modalities and show that BPI

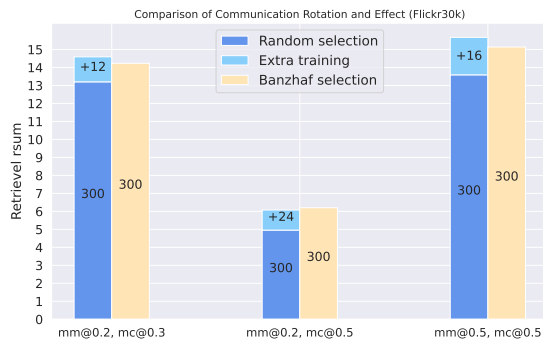


Figure 2: The number of additional training rounds needed for the Random Client Selection to achieve the same performance as the Banzhaf Client Selection (Flickr30k). The blue bar means random selection, and the yellow represents the BPI selection.

achieves higher efficiency than random selection. The Banzhaf client selection strategy aimed to optimize global aggregation efficiency by minimizing communication rounds. Figure 2 illustrates the comparison of communication rounds and performance between the setting with Banzhaf client selection and random client selection across three levels of missing modality. We used Flickr30k dataset in this evaluation. It should be noted that randomly selected patterns required additional (12, 24, or 16) training rounds to surpass or approach the performance of the Banzhaf client selection. To some extent, MMiC facilitates faster convergence of the global model under missing modality settings by prioritizing the selection of core clients.

5.6 MPO: A Potent Solution against Over-fitting

In this section, we show additional features of MPO against overfitting. We only implemented MMiC with MPO and deactivated PPS and BPI. Therefore, the comparison is between $FedAdagrad_{MPO}$ (MMiC) and $FedAdagrad$ (FedOpt) on dataset CrisisMMD (mm@0.2, mc@0.3). Our purpose is to evaluate how the dynamic updating of parameters in $FedAdagrad_{MPO}$ contributes to enhanced stability. During the training, it had been converged after 400 rounds. We continued the training after 400 rounds while observing the personalized performance of $FedAdagrad$ and $FedAdagrad_{MPO}$, which showed the stability of our algorithm. The personalized evaluation is based on the average weighted performance of each client. It can be observed that the personalized performance of FedOpt begins to decline after round 413 and never recovers to its peak level thereafter. This indicated that some clients have already experienced overfitting, leading to a degradation in performance. In contrast, although the performance curve of MMiC experiences a short decline after round 543 as shown in Figure 3. $FedAdagrad_{MPO}$ forms risk by calculating the covariance of historical multi-round returns between pairs of clients (Equation 12). When partial clients overfit, the covariance increases, leading to a higher risk and an overall increase in RARC. When the majority of clients overfit, the total return decreases, yet the overall RARC still increases. An increase in RARC indicates that fewer parameters will be aggregated to the

global model. The experimental results demonstrated that the stability of our algorithm is significantly enhanced by incorporating the MPO, particularly in mitigating performance degradation caused by overfitting during the training of clients.

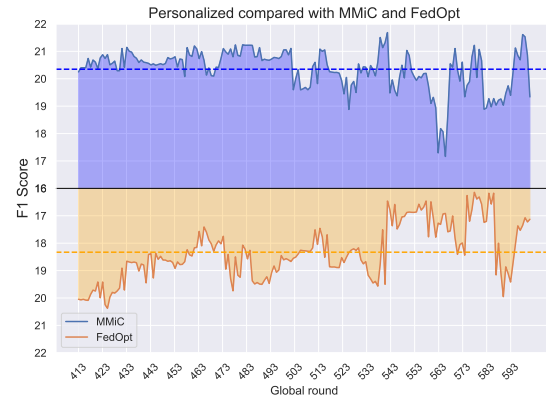


Figure 3: Personalized performance of comparison after continuous training since the model convergence (400 rounds). The two dotted lines are the average scores. The upper part (blue) represents $FedAdagrad_{MPO}$ (MMiC) and the lower part (yellow) represents $FedAdagrad$ (FedOpt).

5.7 Global Performance Influenced by Clustered Federated Algorithms

We explored the impact of clustering quality on MMiC performance. Figure 4 plots *Silhouette Coefficient Value (SCV)* of two clustering algorithms with two different hyperparameters respectively. This experiment was conducted on dataset CrisisMMD (mm@0.2, mc@0.5) and we investigated how to change clustering hyperparameters to get a higher SCV. The SCV quantifies the ratio of the intra-cluster distance, defined as the distance from the sample point to the nearest cluster to which it doesn't belong [42]. A larger SCV signifies a greater separation between the cluster structure containing the sample point and its nearest neighbouring cluster structure, thereby indicating superior clustering quality under these conditions. For Locality Sensitive Hashing (LSH) clustering, their clustering algorithm is based on KMeans [19], which requires specifying the number of clusters. We adjusted the number of clusters from 1 to 20 to identify the two highest SCV. When the number of clusters is set to 3, the SCV attained its peak at 0.185. With 7 clusters and its second highest value of 0.125. For Singular Value Decomposition (SVD) clustering, which employs hierarchical clustering [17], we varied the threshold from 1 to 20 to determine the optimal thresholds, identifying two values: 10 (SCV = 0.18) and 14 (SCV = 0.2). This preliminary selection of clustering parameters assisted us in identifying better and more suitable clustering algorithms and parameters for MMiC.

Figure 5 investigated the selection process of our clustering strategies. What we found are: (1) It's shown that Poverty Parameter Substitution within clusters heavily relies on the quality of client clustering. For instance, in LSH clustering, a higher clustering quality (a higher SCV) often correlates with better global

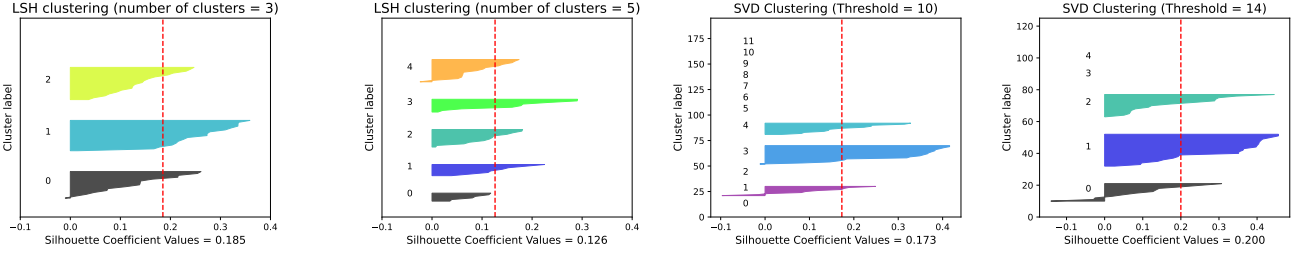


Figure 4: The two plots on the left depict the SCV of LSH clustering under two different hyperparameter (number of clusters), while the two plots on the right show the SCV of SVD-based clustering with the threshold hyperparameter. The numbers within the images represent the indices of the cluster labels.

performance (LSH: 0.185 compared with LSH: 0.126). (2) By comparing different clustering methods, we can infer the contribution of each clustering algorithm to MMiC based on global performance. It is evident that LSH clustering outperformed SVD 0.2 in terms of global model performance when the SCV reached at 0.185. (3) We included manual clustering as a gold standard (clustering based on the overlap of client labels). Overall, both LSH (0.185) and SVD (0.2) clustering achieved global model performance comparable to that of manual clustering, making them reliable references for the clustering algorithms employed in this study. When compared to SVD, LSH demonstrated slightly superior performance.

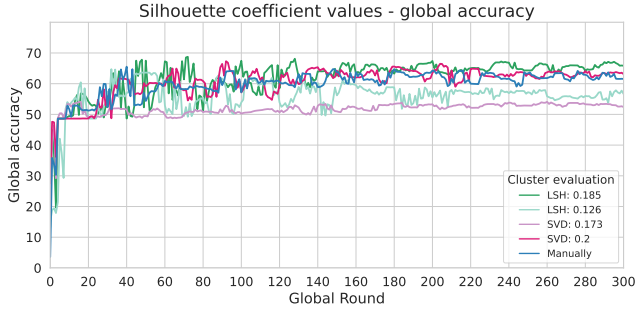


Figure 5: We compared two clustering algorithms, LSH and SVD, by selecting the top-2 SCV hyperparameters for each and evaluating their global performance on MMiC. The blue curve is manual clustering.

5.8 Time Complexity of MPO

Since the Banzhaf Client Selection do not incur an additional cost, the time complexity of MMiC compared to other works depended on the complexity of Markowitz Portfolio Optimization. The aggregation process of $FedAdagrad_{MPO}$ involves the computation of RARC in each cluster, which is then uploaded to the server. The server utilizes the RARC of each cluster to dynamically adjust the beta parameter for aggregation. Since the computational complexity of beta is linear and negligible, the overall complexity of MPO is primarily dominated by the RARC computation. The time complexity of MPO is $O(\frac{K^2}{M} \cdot T + K \cdot T)$. Here we deduce:

- We got average $\frac{K}{M}$ clients for each cluster. Time complexity of σ_{ij} was $O(T)$.

Time complexity of risk $\bar{\sigma}$:

$$\bar{\sigma} = \sum_{i=1}^{\frac{K}{M}} \sum_{j=1}^{\frac{K}{M}} w_i w_j \sigma_{ij}.$$

could be obtained from:

$$O\left(\left(\frac{K}{M}\right)^2\right) \times O(T) = O\left(\left(\frac{K}{M}\right)^2 \cdot T\right)$$

In the covariance σ_{ij} section, we can employ the concept of *prefix sums* [2] to efficiently store historical data. The time complexity of constructing prefix sums was extra $O(\frac{K^2}{M^2})$.

- Hence this part could be improved to $O(\frac{K^2}{M^2}) + O(\frac{K^2}{M^2})$.
- Return A computation is to do the weighted sum for each cluster, and the time complexity of A is $O(\frac{K}{M})$ to each cluster.
- M clusters will upload their RARC to the server and calculate the weighted sum:

$$\left(O\left(\frac{K^2}{M^2} + \frac{K}{M}\right) + O\left(\frac{K^2}{M^2}\right)\right) \times M = O\left(\frac{K^2}{M} + K\right) + O\left(\frac{K^2}{M}\right)$$

Meanwhile, MMiC has a total T global rounds. As *prefix sums* only build at once, we got:

$$O\left(\frac{K^2}{M} + K\right) \times T + O\left(\frac{K^2}{M}\right) = O\left(\frac{K^2 \cdot T}{M} + K \cdot T + \frac{K^2}{M}\right)$$

$O(\frac{K^2}{M})$ was less than $O(\frac{K^2 \cdot T}{M})$ apparently. Therefore, the time complexity of MPO is $O(\frac{K^2}{M} \cdot T + K \cdot T)$.

6 Conclusions

In this work, we introduce MMiC, a model-independent and modality-agnostic framework designed to mitigate the impact of missing modalities in multimodal federated learning. By substituting parameters within clustered federated learning, adapting the Banzhaf Power Index for client selection, and extending Markowitz Portfolio Optimization for global aggregation, MMiC demonstrates improved performance over existing federated architectures in addressing missing modalities. Moving forward, we plan to further enhance the framework's robustness by substituting additional poverty parameters and exploring more efficient solutions.

7 GenAI Usage Disclosure

The authors acknowledge the use of an AI language model to assist in the linguistic refinement of selected sections of this paper, specifically the Introduction and Methodology. All the wordings, equations, and conclusions were revised again after being reviewed by the authors.

References

- [1] Guangyin Bao, Qi Zhang, Duoqian Miao, Zixuan Gong, Liang Hu, Ke Liu, Yang Liu, and Chongyang Shi. 2024. Multimodal Federated Learning with Missing Modality via Prototype Mask and Contrast. arXiv:2312.13508 [cs.LG] <https://arxiv.org/abs/2312.13508>
- [2] Guy E Blelloch. 1990. Prefix sums and their applications. (1990).
- [3] Liwei Che, Jiaqi Wang, Yao Zhou, and Fenglong Ma. 2023. Multimodal Federated Learning: A Survey. *Sensors* 23, 15 (2023). doi:10.3390/s23156986
- [4] Jiayi Chen and Aidong Zhang. 2022. FedMSplit: Correlation-Adaptive Federated Multi-Task Learning across Multimodal Split Networks. In *Proceedings of the 28th ACM SIGKDD Conference on Knowledge Discovery and Data Mining (KDD '22)*.
- [5] Yae Jee Cho, Jianyu Wang, and Gauri Joshi. 2020. Client Selection in Federated Learning: Convergence Analysis and Power-of-Choice Selection Strategies. *CoRR* abs/2010.01243 (2020).
- [6] Don Kurian Dennis, Tian Li, and Virginia Smith. 2021. Heterogeneity for the Win: One-Shot Federated Clustering. In *Proceedings of the 38th International Conference on Machine Learning, ICML 2021, 18-24 July 2021, Virtual Event (Proceedings of Machine Learning Research, Vol. 139)*, Marina Meila and Tong Zhang (Eds.). PMLR, 2611–2620.
- [7] Pradeep Dubey and Lloyd S. Shapley. 1979. Mathematical Properties of the Banzhaf Power Index. *Math. Oper. Res.* 4, 2 (1979), 99–131.
- [8] Fartash Faghri, David J. Fleet, Jamie Ryan Kiros, and Sanja Fidler. 2018. VSE++: Improving Visual-Semantic Embeddings with Hard Negatives. In *Proceedings of the British Machine Vision Conference 2018, BMVC 2018, Newcastle, UK, September 3-6, 2018*. BMVA Press, 12.
- [9] Alireza Fallah, Aryan Mokhtari, and Asuman Ozdaglar. 2020. Personalized Federated Learning with Theoretical Guarantees: A Model-Agnostic Meta-Learning Approach. In *Proceedings of the Advances in Neural Information Processing Systems, NeurIPS 2020, H. Larochelle, M. Ranzato, R. Hadsell, M.F. Balcan, and H. Lin (Eds.)*, Vol. 33. Curran Associates, Inc., 3557–3568. https://proceedings.neurips.cc/paper_files/paper/2020/file/24389bfe4fe2eba8bf9aa9203a44cdad-Paper.pdf
- [10] Tiantian Feng, Digbalay Bose, Tuo Zhang, Rajat Hebbar, Anil Ramakrishna, Rahul Gupta, Mi Zhang, Salman Avestimehr, and Shrikanth Narayanan. 2023. FedMultimodal: A Benchmark for Multimodal Federated Learning. In *Proceedings of the 29th ACM SIGKDD Conference on Knowledge Discovery and Data Mining, KDD 2023, Long Beach, CA, USA, August 6-10, 2023*. ACM, 4035–4045.
- [11] Ignazio Gallo, Gianmarco Ria, Nicola Landro, and Riccardo La Grassa. 2020. Image and Text fusion for UPMC Food-101 using BERT and CNNs. In *Proceedings of the 35th International Conference on Image and Vision Computing New Zealand, IVCNZ 2020, Wellington, New Zealand, November 25-27, 2020*. IEEE, 1–6.
- [12] Avishek Ghosh, Jichan Chung, Dong Yin, and Kannan Ramchandran. 2020. An Efficient Framework for Clustered Federated Learning. In *Proceedings of Advances in Neural Information Processing Systems 33: Annual Conference on Neural Information Processing Systems 2020, NeurIPS 2020, December 6-12, 2020, virtual*.
- [13] Avishek Ghosh, Justin Hong, Dong Yin, and Kannan Ramchandran. 2019. Robust Federated Learning in a Heterogeneous Environment. *CoRR* abs/1906.06629 (2019). <http://arxiv.org/abs/1906.06629>
- [14] Cyril Goutte and Éric Gaussier. 2005. A Probabilistic Interpretation of Precision, Recall and F-Score, with Implication for Evaluation. In *Proceedings of the 27th European Conference on IR Research, ECIR 2005, Santiago de Compostela, Spain, March 21-23, 2005, Proceedings (Lecture Notes in Computer Science, Vol. 3408)*, David E. Losada and Juan M. Fernández-Luna (Eds.). Springer, 345–359.
- [15] Shubham Gupta, Nandini Saini, Suman Kundu, and Debasis Das. 2024. CrisisKAN: Knowledge-Infused and Explainable Multimodal Attention Network for Crisis Event Classification. In *Proceedings of the 46th European Conference on Information Retrieval, ECIR 2024, Glasgow, UK, March 24-28, 2024, Proceedings, Part II (Lecture Notes in Computer Science, Vol. 14609)*. Springer, 18–33.
- [16] László A Jeni, Jeffrey F Cohn, and Fernando De La Torre. 2013. Facing imbalanced data—recommendations for the use of performance metrics. In *Proceedings of the 2013 Humaine association conference on affective computing and intelligent interaction*. IEEE, 245–251.
- [17] Stephen C Johnson. 1967. Hierarchical clustering schemes. *Psychometrika* 32, 3 (1967), 241–254.
- [18] Georgios Kaissis, Marcus R. Makowski, Daniel Rueckert, and Rickmer Braren. 2020. Secure, privacy-preserving and federated machine learning in medical imaging. *Nat. Mach. Intell.* 2, 6 (2020), 305–311.
- [19] Tapas Kanungo, David M Mount, Nathan S Netanyahu, Christine D Piatko, Ruth Silverman, and Angela Y Wu. 2002. An efficient k-means clustering algorithm: Analysis and implementation. *IEEE transactions on pattern analysis and machine intelligence* 24, 7 (2002), 881–892.
- [20] Diederik P. Kingma and Jimmy Ba. 2015. Adam: A Method for Stochastic Optimization. In *Proceedings of the 3rd International Conference on Learning Representations, ICLR 2015, San Diego, CA, USA, May 7-9, 2015, Conference Track Proceedings*.
- [21] Annick Laruelle and Federico Valenciano. 2001. Shapley-Shubik and Banzhaf Indices Revisited. *Math. Oper. Res.* 26, 1 (2001), 89–104.
- [22] Kuang-Huei Lee, Xi Chen, Gang Hua, Houdong Hu, and Xiaodong He. 2018. Stacked Cross Attention for Image-Text Matching. In *Proceedings of the 15th European Conference on Computer Vision, ECCV 2018 (Lecture Notes in Computer Science, Vol. 11208)*. Springer, 212–228.
- [23] Xiang Li, Kaixuan Huang, Wenhao Yang, Shusen Wang, and Zhihua Zhang. 2020. On the Convergence of FedAvg on Non-IID Data. In *Proceedings of the 8th International Conference on Learning Representations, ICLR 2020, Addis Ababa, Ethiopia, April 26-30, 2020*. OpenReview.net. <https://openreview.net/forum?id=HJxNANvTDS>
- [24] Xiaopeng Li, Shasha Li, Shezheng Song, Jing Yang, Jun Ma, and Jie Yu. 2024. Pmet: Precise model editing in a transformer. In *Proceedings of the AAAI Conference on Artificial Intelligence*, Vol. 38. 18564–18572.
- [25] Zichang Liu, Zhaozhuo Xu, Benjamin Coleman, and Anshumali Shrivastava. 2023. One-Pass Distribution Sketch for Measuring Data Heterogeneity in Federated Learning. In *Proceedings of the Advances in Neural Information Processing Systems 36: Annual Conference on Neural Information Processing Systems 2023, NeurIPS 2023, New Orleans, LA, USA, December 10 - 16, 2023*.
- [26] Yunlong Lu, Xiaohong Huang, Yueyue Dai, Sabita Maharjan, and Yan Zhang. 2020. Blockchain and Federated Learning for Privacy-Preserved Data Sharing in Industrial IoT. *IEEE Trans. Ind. Informatics* 16, 6 (2020), 4177–4186.
- [27] Yishay Mansour, Mehryar Mohri, Jae Ro, and Ananda Theertha Suresh. 2020. Three Approaches for Personalization with Applications to Federated Learning. *CoRR* abs/2002.10619 (2020).
- [28] Harry M Markowitz. 1991. Foundations of portfolio theory. *The journal of finance* 46, 2 (1991), 469–477.
- [29] Brendan McMahan, Eider Moore, Daniel Ramage, Seth Hampson, and Blaise Agüera y Arcas. 2017. Communication-Efficient Learning of Deep Networks from Decentralized Data. In *Proceedings of the 20th International Conference on Artificial Intelligence and Statistics, AISTATS 2017, 20-22 April 2017, Fort Lauderdale, FL, USA (Proceedings of Machine Learning Research, Vol. 54)*, Aarti Singh and Xiaojin (Jerry) Zhu (Eds.). PMLR, 1273–1282.
- [30] Merton H. Miller. 1960. Portfolio selection: efficient diversification of investments. *The Journal of Business* 33, 4 (1960), 391–393. <http://www.jstor.org/stable/2350928>
- [31] Takayuki Nishio and Ryo Yonetani. 2019. Client Selection for Federated Learning with Heterogeneous Resources in Mobile Edge. In *Proceedings of 2019 IEEE International Conference on Communications, ICC 2019, Shanghai, China, May 20-24, 2019*. IEEE, 1–7.
- [32] Ferda Ofli, Firoj Alam, and Muhammad Imran. 2020. Analysis of Social Media Data using Multimodal Deep Learning for Disaster Response. In *Proceedings of the 17th International Conference on Information Systems for Crisis Response and Management, ISCRAM 2020, May 2020*. ISCRAM Digital Library, 802–811.
- [33] Shiva Raj Pokhrel and Jinho Choi. 2020. Federated Learning With Blockchain for Autonomous Vehicles: Analysis and Design Challenges. *IEEE Trans. Commun.* 68, 8 (2020), 4734–4746.
- [34] Petra Poklukar, Miguel Vasco, Hang Yin, Francisco S. Melo, Ana Paiva, and Danica Kragic. 2022. Geometric Multimodal Contrastive Representation Learning. In *Proceedings of the International Conference on Machine Learning, ICML 2022, 17-23 July 2022, Baltimore, Maryland, USA (Proceedings of Machine Learning Research, Vol. 162)*. PMLR, 17782–17800.
- [35] Fan Qi and Shuai Li. 2024. Adaptive hyper-graph aggregation for modality-agnostic federated learning. In *Proceedings of the IEEE/CVF Conference on Computer Vision and Pattern Recognition*.
- [36] Alec Radford, Jong Wook Kim, Chris Hallacy, Aditya Ramesh, Gabriel Goh, Sandhini Agarwal, Girish Sastry, Amanda Askell, Pamela Mishkin, Jack Clark, Gretchen Krueger, and Ilya Sutskever. 2021. Learning Transferable Visual Models From Natural Language Supervision. In *Proceedings of the 38th International Conference on Machine Learning, ICML 2021, 18-24 July 2021, Virtual Event (Proceedings of Machine Learning Research, Vol. 139)*. PMLR, 8748–8763.
- [37] Amin Rasekh, Chien-An Chen, and Yan Lu. 2014. Human activity recognition using smartphone. *arXiv preprint arXiv:1401.8212* (2014).
- [38] Sashank J. Reddi, Zachary Charles, Manzil Zaheer, Zachary Garrett, Keith Rush, Jakub Konečný, Sanjiv Kumar, and Hugh Brendan McMahan. 2021. Adaptive Federated Optimization. In *Proceedings of the 9th International Conference on Learning Representations, ICLR 2021, Virtual Event, Austria, May 3-7, 2021*.
- [39] Sashank J. Reddi, Zachary Charles, Manzil Zaheer, Zachary Garrett, Keith Rush, Jakub Konečný, Sanjiv Kumar, and Hugh Brendan McMahan. 2021. Adaptive Federated Optimization. In *Proceedings of the 9th International Conference on Learning Representations, ICLR 2021, Virtual Event, Austria, May 3-7, 2021*. OpenReview.net.

- [40] Yichen Ruan and Carlee Joe-Wong. 2022. FedSoft: Soft Clustered Federated Learning with Proximal Local Updating. In *Proceedings of the 36th AAAI Conference on Artificial Intelligence, AAAI 2022, Thirty-Fourth Conference on Innovative Applications of Artificial Intelligence, IAAI 2022, The Twelveth Symposium on Educational Advances in Artificial Intelligence, EAAI 2022 Virtual Event, February 22 - March 1, 2022*. AAAI Press, 8124–8131.
- [41] Chitwan Saharia, William Chan, Saurabh Saxena, Lala Li, Jay Whang, Emily L. Denton, Seyed Kamyar Seyed Ghasemipour, Raphael Gontijo Lopes, Burcu Karagol Ayan, Tim Salimans, Jonathan Ho, David J. Fleet, and Mohammad Norouzi. 2022. Photorealistic Text-to-Image Diffusion Models with Deep Language Understanding. In *Proceedings of the Advances in Neural Information Processing Systems 35: Annual Conference on Neural Information Processing Systems 2022, NeurIPS 2022, New Orleans, LA, USA, November 28 - December 9, 2022*.
- [42] Ketan Rajshekhar Shahapure and Charles Nicholas. 2020. Cluster Quality Analysis Using Silhouette Score. In *Proceedings of the 7th IEEE International Conference on Data Science and Advanced Analytics, DSAA 2020, Sydney, Australia, October 6-9, 2020*. IEEE, 747–748.
- [43] Niloy Sikder and Abdullah-Al Nahid. 2021. KU-HAR: An open dataset for heterogeneous human activity recognition. *Pattern Recognition Letters* 146 (2021), 46–54.
- [44] Virginia Smith, Chao-Kai Chiang, Maziar Sanjabi, and Ameet Talwalkar. 2017. Federated Multi-Task Learning. In *Proceedings of Advances in Neural Information Processing Systems 30: Annual Conference on Neural Information Processing Systems 2017, December 4-9, 2017, Long Beach, CA, USA*. 4424–4434.
- [45] Alysa Ziyang Tan, Han Yu, Lizhen Cui, and Qiang Yang. 2023. Towards Personalized Federated Learning. *IEEE Trans. Neural Networks Learn. Syst.* 34, 12 (2023), 9587–9603. <https://doi.org/10.1109/TNNLS.2022.3160699>
- [46] Yee Whye Teh. 2010. Dirichlet Process. In *Encyclopedia of Machine Learning*, Claude Sammut and Geoffrey I. Webb (Eds.). Springer, 280–287.
- [47] Saeed Vahidian, Mahdi Morafah, Weijia Wang, Vyacheslav Kungurtsev, Chen Chen, Mubarak Shah, and Bill Lin. 2023. Efficient Distribution Similarity Identification in Clustered Federated Learning via Principal Angles between Client Data Subspaces. In *Proceedings of the 37th AAAI Conference on Artificial Intelligence, AAAI 2023, Thirty-Fifth Conference on Innovative Applications of Artificial Intelligence, IAAI 2023, Thirteenth Symposium on Educational Advances in Artificial Intelligence, EAAI 2023, Washington, DC, USA, February 7-14, 2023*. AAAI Press, 10043–10052.
- [48] Shiqiang Wang and Mingyue Ji. 2024. A Lightweight Method for Tackling Unknown Participation Statistics in Federated Averaging. In *Proceedings of The 12th International Conference on Learning Representations, ICLR 2024, Vienna, Austria, May 7-11, 2024*. OpenReview.net.
- [49] Qiong Wu, Kaiwen He, and Xu Chen. 2020. Personalized Federated Learning for Intelligent IoT Applications: A Cloud-Edge Based Framework. *IEEE Open J. Comput. Soc.* 1 (2020), 35–44.
- [50] Renjie Wu, Hu Wang, and Hsiang-Ting Chen. 2024. A Comprehensive Survey on Deep Multimodal Learning with Missing Modality. *CoRR abs/2409.07825* (2024). arXiv:2409.07825 doi:10.48550/ARXIV.2409.07825
- [51] Baochen Xiong, Xiaoshan Yang, Yaguang Song, Yaowei Wang, and Changsheng Xu. 2023. Client-Adaptive Cross-Model Reconstruction Network for Modality-Incomplete Multimodal Federated Learning. In *Proceedings of the 31st ACM International Conference on Multimedia (MM), MM 2023, Ottawa, ON, Canada, 29 October 2023- 3 November 2023*. ACM, 1241–1249.
- [52] Lishan Yang, Alireza Seyed Shakeri, Liangxi Pu, Weitong Chen, and Yanjun Shu. 2024. Efficient Clustered Federated Learning by Locality Sensitive Hashing. In *International Conference on Advanced Data Mining and Applications*. Springer, 177–191.
- [53] Peter Young, Alice Lai, Micah Hodosh, and Julia Hockenmaier. 2014. From image descriptions to visual denotations: New similarity metrics for semantic inference over event descriptions. *Trans. Assoc. Comput. Linguistics* 2 (2014), 67–78.
- [54] Qiyang Yu, Yang Liu, Yimu Wang, Ke Xu, and Jingjing Liu. 2023. Multimodal Federated Learning via Contrastive Representation Ensemble. In *Proceedings of the 11th International Conference on Learning Representations, ICLR 2023, Kigali, Rwanda, May 1-5, 2023*. OpenReview.net.
- [55] Songcan Yu, Junbo Wang, Walid Hussein, and Patrick C. K. Hung. 2024. Robust multimodal federated learning for incomplete modalities. *Comput. Commun.* 214 (2024), 234–243. <https://doi.org/10.1016/j.comcom.2023.12.003>
- [56] Linlin Zong, Qiuqie Xie, Jiahui Zhou, Peiran Wu, Xianchao Zhang, and Bo Xu. 2021. FedCMR: Federated Cross-Modal Retrieval. In *Proceedings of the 44th International ACM SIGIR Conference on Research and Development in Information Retrieval, Virtual Event, Canada, July 11-15, 2021*. ACM, 1672–1676.